Contents

This page intentionally left blank

Appendix A

Description of code and data

Following the standards set out by Irving (2016), special care was taken to ensure the reproducibility of the results in this thesis and enable others to use and extend the code in the future.

A.1 Raw data availability

All the raw data needed to produce the results are publicly available on Zenodo. They amount to approximately 109 GB in total and have been divided between the following records:

1. https://doi.org/10.5281/zenodo.10090744
2. https://doi.org/10.5281/zenodo.10093567
3. https://doi.org/10.5281/zenodo.10094438

The vast majority of the data is model output in netCDF format, which can be accessed using the `xarray` package in Python. Each output dataset is accompanied by a human-readable log file listing the parameter settings used.

A.2 Code description

The code and all other material needed to reproduce the results are publicly available on GitHub at https://github.com/tschanzer/honours-project. The repository is centred around the package named `modules`, which contains four Python modules:

- `modules.models` contains the code needed to run the simulations. It defines a class `Model` for running normal simulations and a class `SingleStepModel` for applying single time steps in order to calculate subgrid tendencies. The governing equations are specified when instantiating these classes by passing custom "equation classes" as arguments. Equation classes for the parametrised and unparametrised simulations in this thesis have already been implemented, and new (e.g., stochastic) parametrisation schemes can be created and coupled into the models by simply defining new equation classes.
- `modules.coarse_graining` defines a `CoarseGrainer` class that implements the coarse-graining operation described in Chapter 4.
- `modules.stats` provides functions for calculating metrics such as the Nusselt number that are used to analyse the solutions.

- `modules.tools` provides other useful analysis functions.

All functions, methods and classes are annotated with docstrings explaining their usage in detail.

A.3 Instructions for reproducing the results

The results and figures shown in this thesis may be reproduced by first following the instructions at https://github.com/tschanzer/honours-project#readme to set up the virtual environment and data directories, and then running the Python notebooks in the `final_notebooks` directory of the repository.

It is also possible to generate the raw data from scratch. The model settings used in this work are recorded in human-readable YAML configuration files in the `config` directory of the repository. Simulations using these settings can be run by executing the scripts in the `scripts` directory of the repository, passing a configuration file as a command line argument like so:

```
$ mpiexec -n <ncpus> python -m mpi4py scripts/run_model.py <config file>.yml
```

Further assistance is available upon request.

Appendix B

Details of numerical experiments

B.1 Initial condition

The initial velocity field is specified in terms of the streamfunction (whose level curves are streamlines of the flow)

$$\psi_0(x,z) = 0.1\sin(\pi x)(1-(2z-1)^2)^2,$$

from which

$$u_0(x,z) = -\frac{\partial\psi_0}{\partial z} \quad \text{and} \quad w_0(x,z) = \frac{\partial\psi_0}{\partial x}.$$

It is easily verified that these satisfy the required boundary conditions. The reason for using the streamfunction is that it guarantees a divergence-free velocity field ($\partial u/\partial x + \partial w/\partial z = -\partial^2\psi/\partial x\partial z + \partial^2\psi/\partial z\partial x \equiv 0$).

The initial temperature field is

$$\theta_0(x,z) = \frac{1}{2}(1-2z)^9$$

plus a random perturbation at each grid point, drawn from the normal distribution with mean zero and height-dependent standard deviation $(1-(2z-1)^2)\times 10^{-2}$. The random perturbation is necessary to break the symmetry that the initial condition would otherwise have.

Figure B.1 shows the initial streamfunction, velocity and temperature fields. There are eight equally-sized counter-rotating convection cells.

B.2 Model spin-up time

It is critical to ensure that the simulations have reached a statistically steady state (to "spin" them up) in order to accurately calculate long-term statistics. To that end, I have calculated the 250-time-unit rolling means of the Nusselt number, thermal boundary layer thickness, RMS speed, kinetic energy dissipation rate and thermal dissipation rate (see § 3.6 for the definitions) using the data from the 1024×128 simulation described in § 3.6. These are plotted in Figure B.2. The RMS speed and kinetic energy dissipation rate take longer than the other variables to reach a steady state and exhibit larger low-frequency oscillations. Nonetheless, I determine that the simulation has reached a sufficiently steady state at $t = 750$.

In the resolution-dependence experiment of § 3.6, the simulations with resolution higher than 1024×128 were initialised by interpolating the 1024×128 solution at time $t = 650$. These also needed to reach a statistically steady state. Figure B.3 shows the 150-time-unit rolling means of the same quantities as Figure B.2 for the 2048×256 simulation. I determine that the means reach a sufficiently steady state

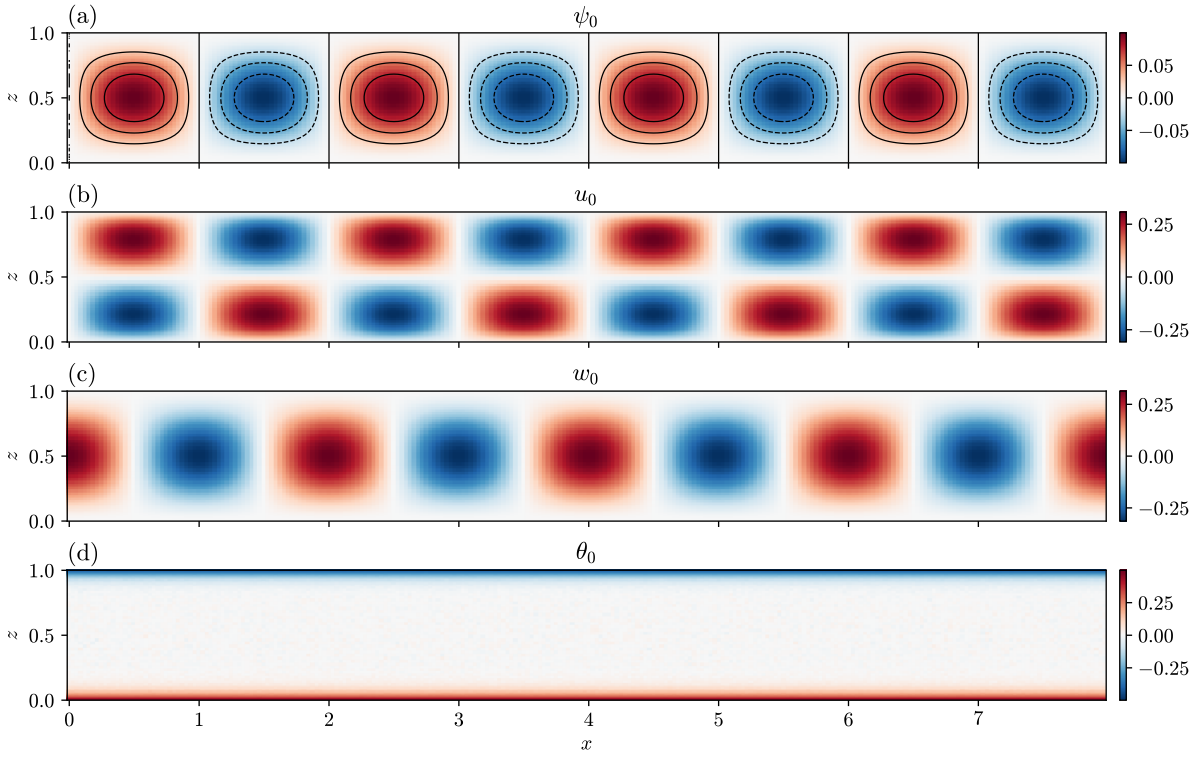

Figure B.1: Initial streamfunction **(a)**, horizontal velocity **(b)**, vertical velocity **(c)** and temperature **(d)**.

when the right edge of the rolling window is at $t = 900$; it is therefore appropriate to use the data from $t = 900 - 150 = 750$ onwards.

B.2.1 Parametrised model spin-up time

The parametrised model described in Chapter 5 was very slow to reach a statistically steady state. Figure B.4 performs the same rolling mean analysis as above with a 250 time unit window; I determine that 800 time units are required.

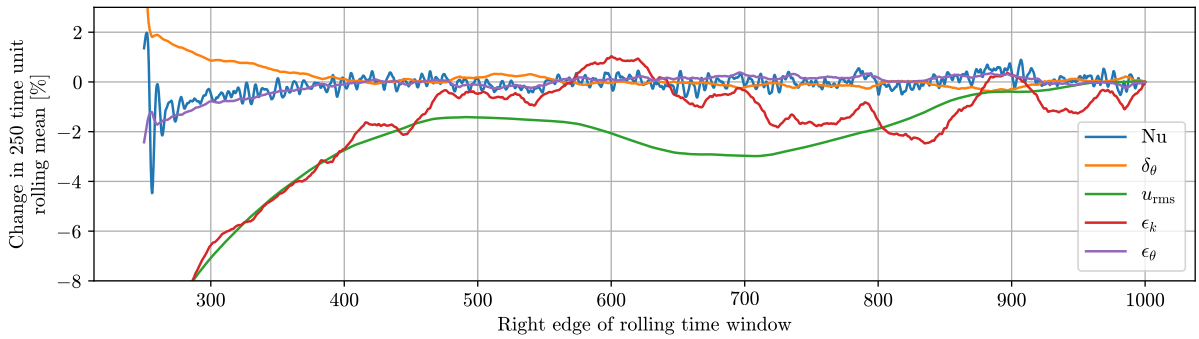

Figure B.2: 250-time-unit rolling means of the Nusselt number Nu, thermal boundary layer thickness δ_θ, RMS speed u_{rms}, kinetic energy dissipation rate ϵ_k and thermal dissipation rate ϵ_θ for the 1024×128 simulation described in § 3.6. The horizontal coordinate is the position of the *right* edge of the rolling window. Each quantity is expressed as a percentage deviation relative to its value when the right edge of the window is at $t = 1000$.

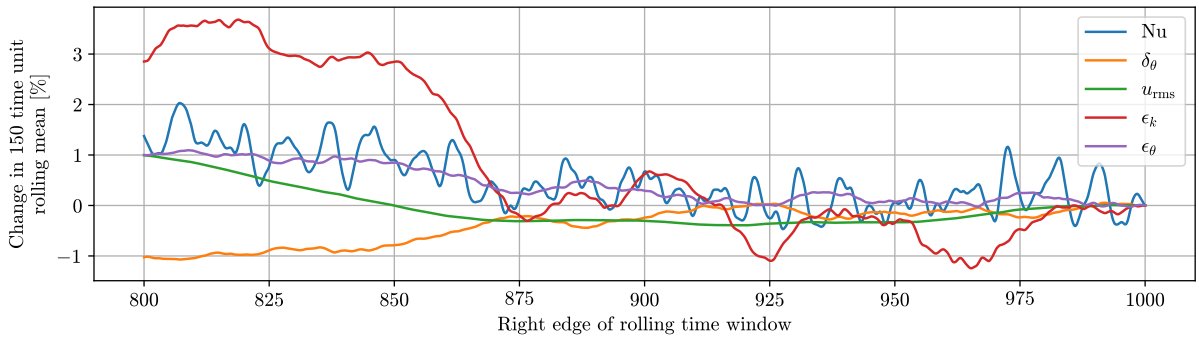

Figure B.3: Similar to Figure B.2, but showing 150-time-unit rolling means for the 2048×256 simulation, which was initialised by interpolating the 1024×128 solution at time $t = 650$.

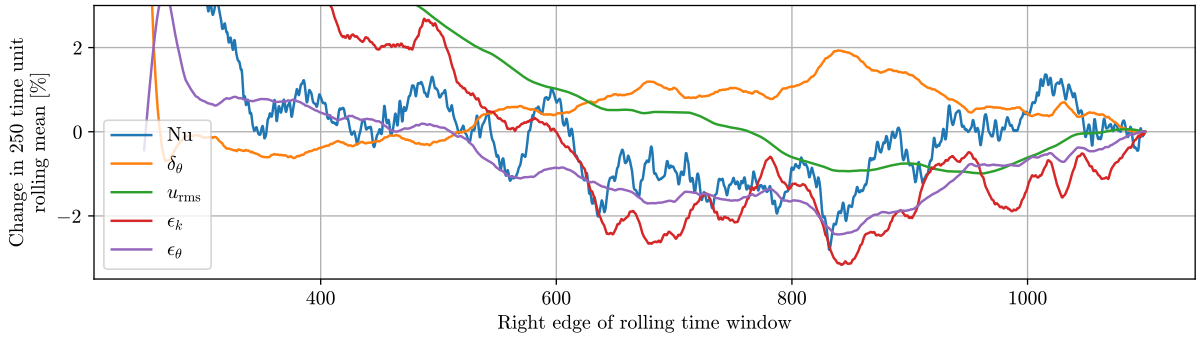

Figure B.4: Similar to Figure B.2, for the parametrised 256×64 simulation.

B.3 Training dataset snapshot frequency

When building the parametrisation training dataset for Chapter 4, the amount of storage space demanded by the high-resolution model output made it desirable to avoid saving redundant information. Saving the model state every time step or every 0.2 time units (as in § 3.6) would waste space and reduce the diversity of the training dataset, because the state exhibits substantial autocorrelation at these intervals. Figure B.5 shows the spatially averaged temporal autocorrelation functions of u, w and θ, computed for the 1024×128 simulation that is described in § 3.6 (again discarding the first 750 time units of data for spin-up). Observing that all three variables reach the first correlation minimum at a lag of approximately 3 time units, I choose to save the model output at this interval.

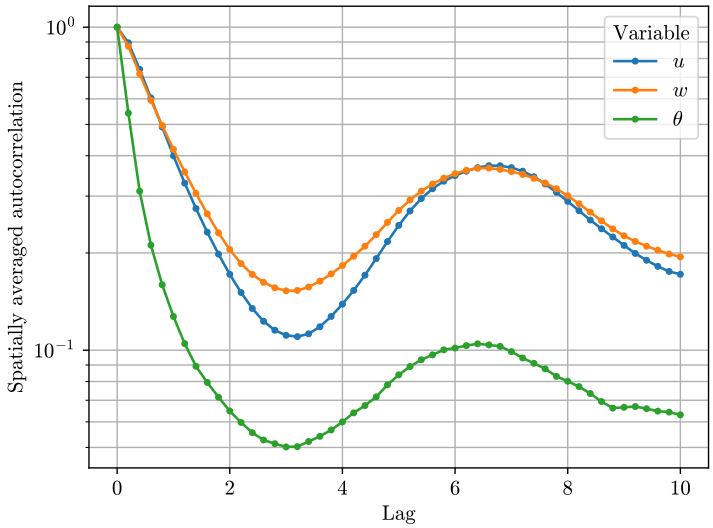

Figure B.5: Spatially averaged autocorrelation functions of the three prognostic variables in the 1024×128 simulation that is described in § 3.6.

Bibliography

Irving, D. (2016). "A minimum standard for publishing computational results in the weather and climate sciences". *Bull. Am. Meteorol. Soc.* **97**(7). DOI: 10.1175/BAMS-D-15-00010.1.